Threading Immobilized DNA Molecules through a Solid-State Nanopore at >100 μs per Base Rate

Changbae Hyun, Harpreet Kaur, Ryan Rollings, Min Xiao, and Jiali Li*

Department of Physics, University of Arkansas, Fayetteville, Arkansas 72701, United States

ABSTRACT In pursuit of developing solid-state nanopore-based DNA sequencing technology, we have designed and constructed an apparatus that can place a DNA-tethered probe tip near a solid-state nanopore, control the DNA moving speed, and measure the ionic current change when a DNA molecule is captured and released from a nanopore. The probe tip's position is sensed and controlled by a tuning fork based feedback force sensor and a nanopositioning system. Using this newly constructed apparatus, a DNA strand moving rate of >100 μs/base or <1 nm/ms in silicon nitride nanopores has been accomplished. This rate is 10 times slower than by manipulating DNA-tethered beads using optical tweezers and 1000 times slower than free DNA translocation through solid-state nanopores reported previously, which provides enough temporal resolution to read each base on a tethered DNA molecule using available single-channel recording electronics on the market today. This apparatus can measure three signals simultaneously: ionic current through a nanopore, tip position, and tip vibrational amplitude during the process of a DNA molecule's capture and release by a nanopore. We show results of this apparatus for measuring λ DNA's capture and release distances and for current blockage signals of λ DNA molecules biotinylated with one end and with both ends tethered to a tip.

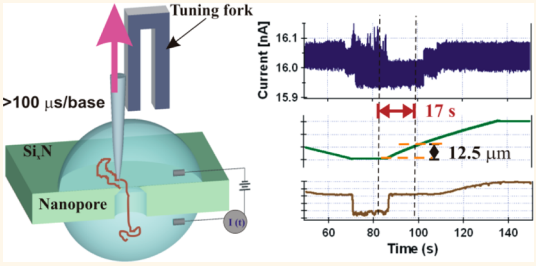

KEYWORDS: solid-state nanopore · DNA · probe tip · tuning fork · tethered DNA translocation · nanopositioning · DNA capture distance

Since voltage-biased protein channels were demonstrated to be capable of detecting single-stranded DNA and RNA molecules 15 years ago,[1] and 5 years later solid-state nanopores were fabricated to overcome the stability and size limitations of protein membrane structures,[2−4] nanopore technology has become a fast increasing field due to its potential application in single-molecule DNA sequencing[5−7] and its applications in characterizing single protein molecules at their native and denatured states.[8−16] When a nanopore in an insulating membrane is immersed in an electrolyte and a voltage is applied across the membrane, the flow of ions through the pore generates an open pore current. A DNA molecule nearby can be captured and driven through by the electric field of the pore. The passing of a DNA molecule partially blocks the flow of ions, producing a current drop event characterized by its magnitude and time duration. Much effort has been devoted to increase both the current drop magnitude and time duration to improve the spatial and temporal resolution of a nanopore device for the ultimate goal of reading DNA sequence electrically and for single-molecule proteomics. These efforts include decreasing nanopore thickness and increasing DNA translocation time.[17−25] In this work, we report a technique developed to overcome one of the major obstacles in nanopore single DNA and protein analysis: controlling the moving speed of a biomolecule in a nanopore by integrating a solid-state nanopore device with a DNA-tethered probe tip that is position-controlled and sensed by a nanopositioning system and a tuning fork based force sensor.

As reviewed by Keyser *et al.*,[22] many research groups have tried to control the speed of DNA transport through a nanopore by modifying the translocating molecule,[26] the nanopore,[27] or mechanically manipulating the DNA molecules.[28,29] Mechanically manipulating DNA molecules has been performed by DNA-tethered beads suspended in solution and controlled either by optical tweezers or by a magnetic trap. The optical

* Address correspondence to jialili@uark.edu.

Received for review March 11, 2013 and accepted June 11, 2013.

Published online June 11, 2013
10.1021/nn4012434

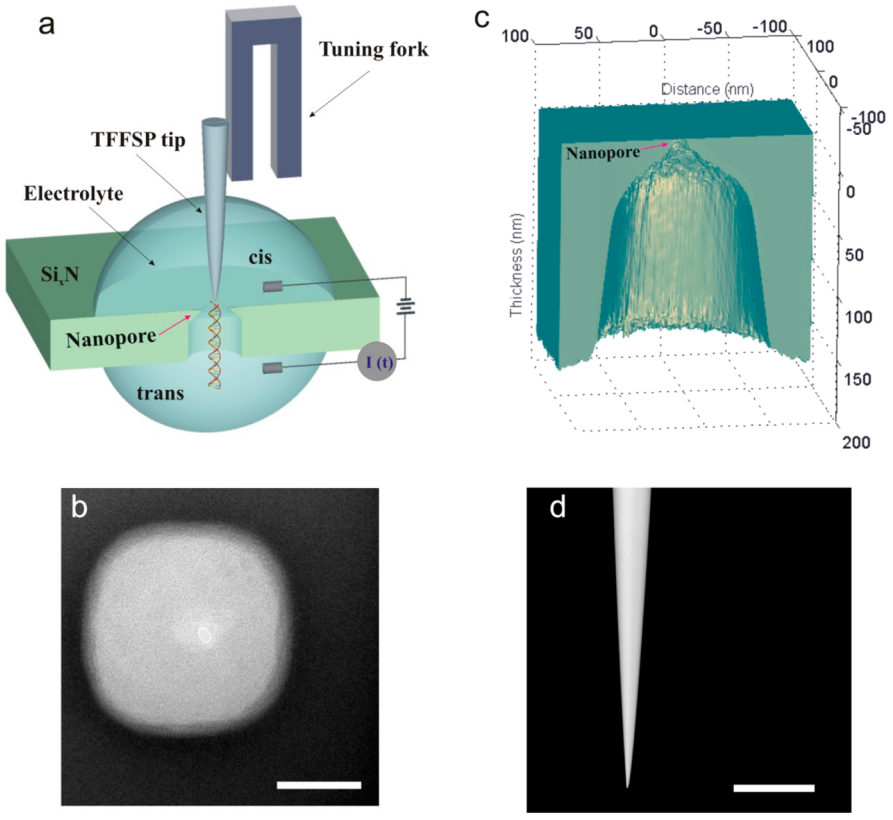

Figure 1. (a) Diagram of the SSN-TFFSP experimental setup (not to scale). A λ DNA is tethered to the TFFSP tip through biotin−streptavidin bonding. The optical fiber tip is glued to one prong of a tuning fork that is attached to a piezo actuator. The piezo actuator is controlled by a *XYZ* piezo positioner (not shown) that controls the location of the tip. (b) TEM image of a nanopore used in this work. The scale bar in the image is 50 nm long. (c) Thickness profile across the nanopore shown in (b). (d) SEM image of an optical fiber tip coated with Cr/Au used in this work. The scale bar is 20 μm long.

tweezers method, which traps a DNA-tethered bead in the crossover of a focused laser beam, can manipulate the DNA-tethered bead in three dimensions and has a pico-newton range of force sensitivity. However, heating due to the laser in optical tweezers increased the ionic current through a nanopore and noise,[30,31] requiring the optically trapped bead to be several micrometers away from a nanopore. Furthermore, the bead trapping methods also have a Brownian motion problem that makes it difficult to control the motion of the bead with less than 10 nm resolution. In contrast, a scanning probe tip in an AFM- or SNOM-based system can approach more closely to a nanopore and can have sub-nanometer spatial resolution as reported recently.[32,33]

Motivated by controlling the speed of DNA translocation in a nanopore at a rate of ~100 μs/base or slower for developing solid-state nanopore-based DNA sequencing technology, we have designed and constructed an apparatus as shown in Figure 1a. This apparatus combines the measurement of ionic current through a solid-state nanopore with a DNA-tethered probe tip that is position-controlled and sensed by a tuning fork force sensor and a nanopositioning system. We report here that by using this newly constructed apparatus that integrates a **S**olid-**s**tate **N**anopore and a **T**uning **F**ork based **F**orce **S**ensing **P**robe tip, SSN-TFFSP, by tethering λ DNA molecules to the probe tip, a DNA translocation speed of ~400 μs/base or 1 nm/ms in a solid-state nanopore has been accomplished. This speed is 10 times slower than the optical trapping DNA-tethered bead method reported[34] and 1000 times slower than free DNA translocation through solid-state nanopores.[4,5,7,35] We will first describe the details of this SSN-TFFSP apparatus. We then show the current blockage traces caused by tethered λ DNA being captured by a nanopore and the process of DNA being pulled out by a TFFSP tip. We show the λ DNA's most probable capture and release distances measured by this SSN-TFFSP system and show that these results are consistent with the radius of gyration and the contour length of λ DNA molecules in solution. Furthermore, we present current blockage signals of λ DNA biotinylated with one end and with both ends tethered to a tip measured by this apparatus.

EXPERIMENTAL SETUP

Figure 1a shows a schematic diagram of the integrated solid-state nanopore and tuning fork force sensor based probing (SSN-TFFSP) system constructed for this work. A DNA molecule is tethered to a TFFSP tip that is glued to one prong of a quartz tuning fork.

The tuning fork is attached to a piezo actuator that is affixed to an *XYZ* piezo positioner (nanopositioner, Mad City Laboratories, not shown in the diagram). The TFFSP tip's position in solution is sensed by the tuning fork sensor and is controlled by the *XYZ* nanopositioner. The vibration amplitude of the tuning fork is sensitive to the viscous drag in solution and the sheer force when the tip is close to a surface. A nanopore chip containing a window of 30 μm free-standing silicon nitride membrane with a ~10 nm pore at its center (Figure 1b shows a TEM image and 1c shows its thickness profile) divides the electrolyte solution into two sections: *cis* and *trans* chambers, which are made of glass sealed with PDMS (not shown). The sole electrical and fluidic connection between the two chambers is the nanopore. The electrolyte solution used in this work is 1 M potassium chloride (KCl) with 10 mM Tris at pH 8. The ionic current through the pore is measured by a pair of Ag/AgCl electrodes in each chamber. The ionic current is measured and recorded with the Axopatch 200B integrated amplifier system (Molecular Devices) with its low pass Bessel filter set at 2 kHz in this work. The sample holder that holds a pair of *cis* and *trans* chambers with a nanopore chip sandwiched between is mounted on a manual *XYZ* micromanipulator. The whole SSN-TFFSP system is shielded by a Faraday cage.

After a nanopore is tested with reasonable open pore current and noise level, the DNA-attached tip is immersed in the *cis* chamber. When the tip is near the nanopore, one or more DNA molecules can be captured by the electric field extended outside of the nanopore[32,33,36,37] and pulled into the nanopore until the captured DNA molecule is stretched and held by the tethering force from the TFFSP tip. A DNA molecule near or inside a nanopore partially blocks the flow of ions, increases the pore resistance, and produces an observable drop in pore current. When the captured DNA molecule is pulled out from the nanopore by the probe tip, the pore current recovers. By observing these current drops and recoveries, the process of capturing and releasing tethered DNA molecules by a nanopore can be measured. Details of the main components of this SSN-TFFSP system, sample preparation, and the experiment to be performed are described in the Methods section.

RESULTS AND DISCUSSION

Figure 2 shows that the integrated SSN-TFFSP system can measure three parameters *versus* time simultaneously: (1) the ionic current through the nanopore (Figure 2a), (2) the tip distance above the membrane surface (Figure 2b), and (3) the vibration amplitude of the tuning fork (Figure 2c). The ionic current in Figure 2a was measured by applying 60 mV across the nanopore shown in Figure 1b. The stable open pore current was 16 $\pm$ 0.7 nA, which was larger than expected from the 10 nm diameter pore shown in Figure 1b. The diameter of the pore in solution was estimated to be about 20 nm judging by the open pore current. Figure 2b shows that the tip's end was initially 32 μm above the nanopore surface. As the tip was approaching the nanopore from the starting time of (i), the vibration amplitude of the tuning fork decreased slightly since the tip's immersion depth increased (Figure 2c). When the probe tip was at ~2 μm distance above the pore at time (ii), a drop in ionic current occurred, indicating possibly that a tethered DNA molecule was captured by the nanopore electric field. When the tip was brought closer to and engaged to the membrane near the pore, its vibration amplitude decreased abruptly at the time of (iii) due to increased shear force (the tip was not right on top of the pore; it was placed a little bit away from the nanopore but within DNA capture distance). The tip stayed on the membrane from the time of (iii) to (v) and started to move up at the beginning of time (v). The current noise increased when the tip was on the membrane (see Figures SI_1−4 and 11 in Supporting Information for more recorded traces), possibly caused by the tip's mechanical vibration that disturbed ionic current flow to the pore. This interpretation is consistent with the observation that this vibration-related current noise was absent before the tip had interacted with the membrane and after the tip had moved up from the membrane. When the tip was at 12.7 and 15.8 μm above the pore, the pore current stepped up with ΔI_2 = 43 pA at (vi) and ΔI_1 = 23 pA at (vii). The ionic current recovered to its original value at time (vii). The tip was lifted to its starting position at time (viii). This experiment, tethered DNA molecules on a probe tip approaching the same nanopore then pulling up by the nanopositioner, was repeated more than 10 times with the same nanopore and tip (see Figures SI_1 to SI_7 in Supporting Information). Most of these measurements show multiple steps of current drop and recovery. The statistics of the first capture and last release distances are shown in Figure 3. The statistics of the magnitudes of the current drop and recovery steps are shown in Figure 4a.

During measurements, parameters were adjusted to avoid biotin−streptavidin rupture.[38] After applying a 500 mV voltage across a nanopore for a few seconds right after a DNA molecule was captured by a nanopore at a 60 mV bias voltage, the DNA capture events could not be measured again, possibly due to the rupture between biotin−streptavidin bonding. The biotin−streptavidin bonding could also break when the tip was pulled too fast even at a 60 mV bias voltage, for example, lifting the tip 10 μm up within 100 ms after a tethered DNA molecule was trapped inside a nanopore.

The DNA's capture distance by the electric field extended outside of a nanopore can be measured in

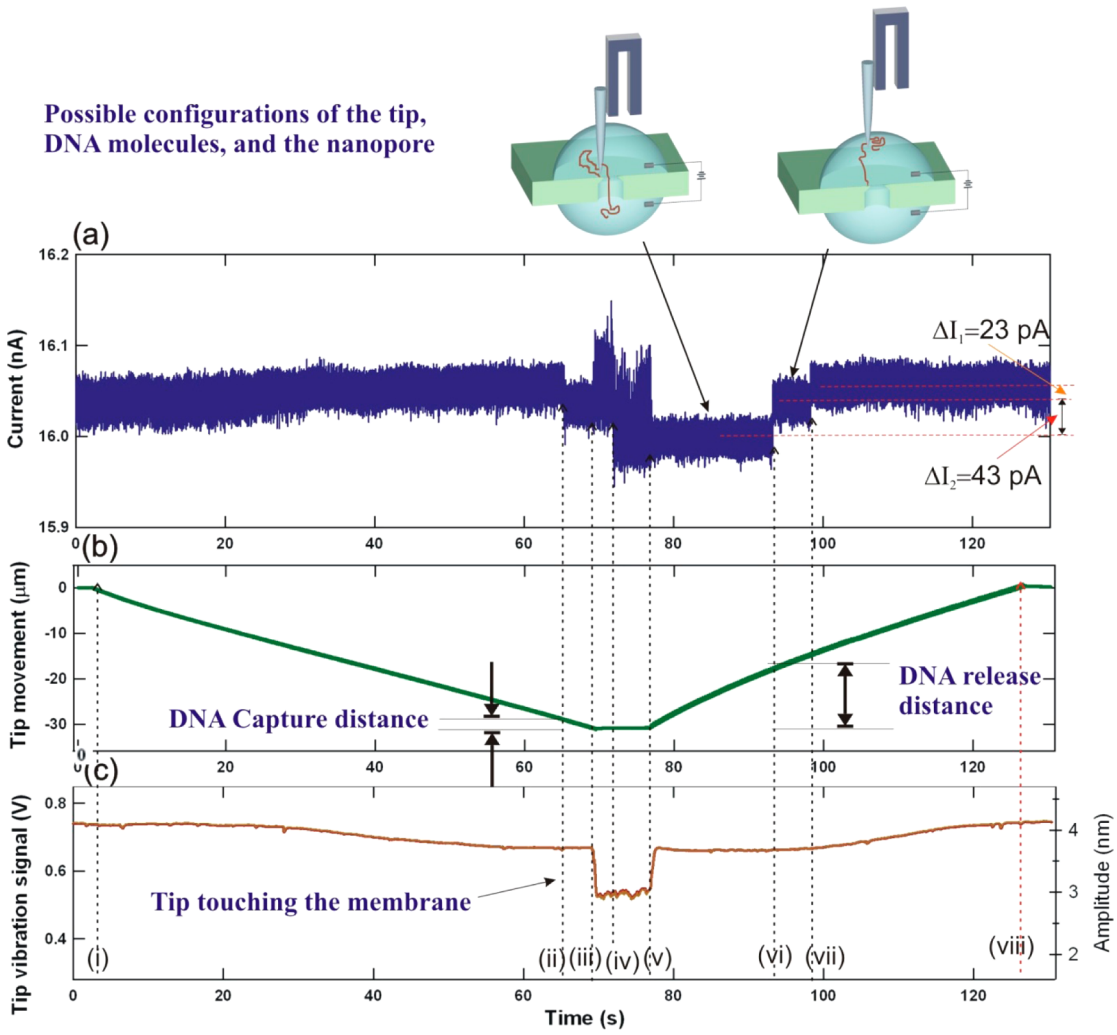

Figure 2. Parameters measured in the SSN-TFFSP apparatus. (a) Current through the nanopore shown in Figure 1b in 1 M KCl solution with 60 mV bias voltage. Current dropped when DNA molecules were captured by the nanopore, and current recovered to its original value when the DNA was released from the nanopore. (b) TFFSP tip's movement. (c) Tuning fork's voltage signal after 1000 times amplification as the tip approaches and lifts from the nanopore surface. The right axis is the vibration amplitude converted by 0.18 V/nm.

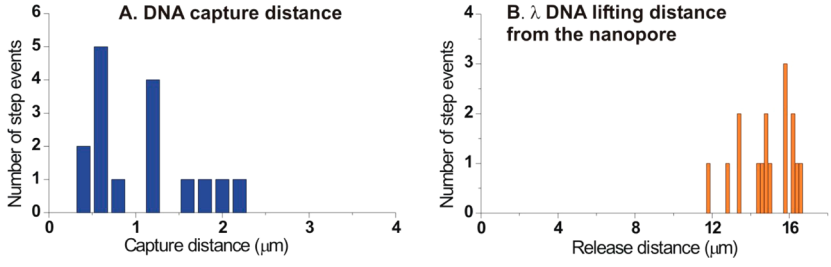

Figure 3. Capture and release distance of λ DNA. (A) DNA's first capture distance from the tip's end to the membrane surface. The capture distance is comparable to λ DNA's gyration radius (500 nm). (B) DNA last release distance when a tip moved away from a nanopore. The averaged last release distance (15.1 μm) is close to λ DNA's contour length (16.4 μm). Data from two more sets of similar experiments are added to this figure to increase the number of step events.

this SSN-TFFSP system in a similar way to those discussed by other groups using optical tweezers.[34,39] At time (ii) in Figure 2, current drop occurred before the tip was engaged to the membrane. The distance moved by the tip between (ii) and (iii) was ~1.8 μm, indicating the capture distance. The measured capture distances in this experiment are shown in Figure 3A. The average of the capture distances in Figure 3A is 1.1 ± 0.6 μm. This value is comparable to λ DNA's radius of gyration, ~1 μm/2 = 0.5 μm. We also measured the tip's moving distance from the starting time of (v) to the time at which DNA was released (vii), as shown in

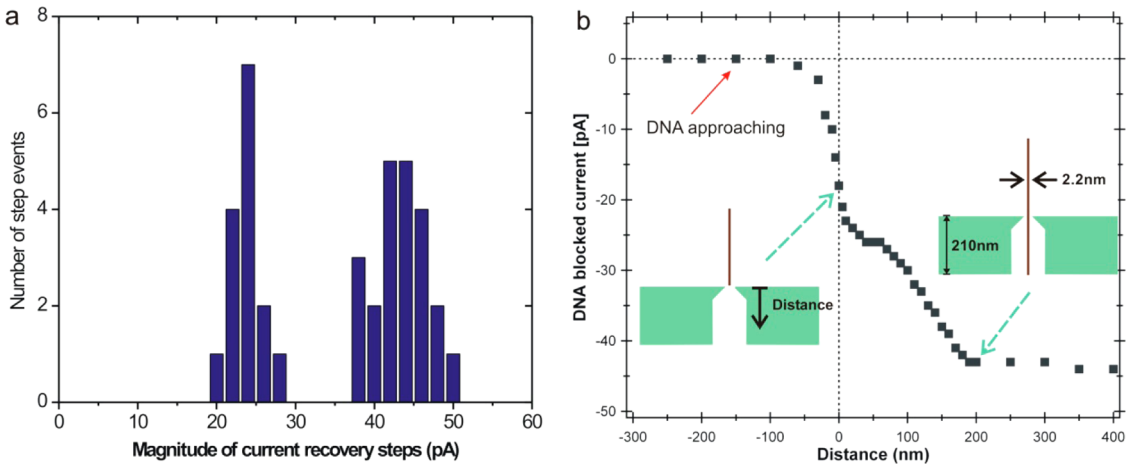

Figure 4. (a) Amplitudes of current recovery step when DNA was pulled up from the nanopore. (b) COMSOL simulation of current blockage by dsDNA *vs* DNA−nanopore distance. Geometry of the nanopore is referred to the thickness profile shown in Figure 1c, and its diameter is 26 nm. DNA is considered as an insulating 2.2 nm diameter cylinder rod. The distance is from the end of the cylinder rod to the top surface of a membrane as shown in the inset. The open pore current for 1 M KCl is I_0 = 14.9 nA in this simulation.

Figure 3B. The average last release distance is about 15.0 ± 1.2 μm, very close to the contour length of a 48.6 kbp λ DNA (16.4 μm) molecule. The spanning time between (v) and (vii) was 21.4 s, thus the DNA translocation speed as it was retracted from the pore was 0.73 μm/s or 1 base/400 μs. This rate is 10 times slower than moving a DNA-tethered bead by optical tweezers reported[34] and 1000 times slower than the reported free DNA translocation through solid-state nanopores.[4,5,7,35] If we set the tip's moving up time from (v) to (viii) to be as slow as the tip's approaching time from (i) to (ii) (Figure 2), the DNA translocation speed in a nanopore could reach as slow as 0.4 μm/s or 1 base/800 μs. Note, the DNA pulling out rate in this SSN-TFFSP system is a user-defined parameter for the nanopositioning system, practically no upper limit.

The time resolution of a nanopore device is determined by the DNA translocation speed and the bandwidth of the current recording electronics. Considering the highest bandwidth for a typical nanopore current recording system available on the market is ~100 kHz (~10 μs), and most published DNA translocation data were recorded at 10 or 100 kHz (~100 μs), the speed of 1 base/400 μs would provide enough temporal resolution to read each base on a tethered DNA molecule. This experiment had demonstrated that the newly constructed SSN-TFFSP system has obtained the time resolution required to electrically read a DNA's sequence.

After DNA was pulled out of the nanopore at the times (v) and (vii) shown in Figure 2, the ionic current recovered to its original open pore value. The amplitudes of current recoveries are shown in Figure 4a. The histogram of the current recoveries in Figure 4a shows two peaks with the average values of 23.8 ± 2.0 and 43.4 ± 3.4 pA instead of a single peak. Considering that the current changes ΔI_2 = 43 pA and ΔI_1 = 23 pA are not the same, and this ΔI_1 = 23 pA was often corresponding to "sticking events" or events with no DNA pulling out process observed from time (v) to (vi) (see Figures SI_8, 9, and 12), we assume that the ΔI_1 = 23 pA was caused by a DNA molecule sticking near the nanopore surface, and the ΔI_2 = 43 pA occurring at (iv) was a real DNA translocation through the nanopore as illustrated at the top of Figure 2. Below we discuss why this assumption is reasonable and why we had observed two or even more steps during the processes of current drop and recovery.

As described in the Methods section of tethering DNA to a tip, many copies of λ DNA can attach to a tip. Therefore, two or more copies of λ DNA molecules could be captured by a nanopore. This is also consistent with our observations shown in Figure 2 and the figures in Supporting Information. To further estimate the approaching process and the amount of current blocked from an approaching DNA at different DNA−nanopore distances, we have simulated the current drop amplitudes using a finite element analysis program (COMSOL, Multiphysics).

To estimate the current drop magnitude induced by a DNA molecule near or inside a nanopore, we have used Nernst−Planck and Poisson equations (COMSOL). The Nernst−Planck equation describes the flux of chemical ions (potassium and chloride ions) under the influence of an electric field in solution under user-defined nanopore geometries. The electrical field and the electrical potential generated in ionic solution are described by the Poisson equation. Using these equations and the nanopore geometry shown in Figure 1c with or without DNA, we can solve for the flux of the chloride ions and potassium ions through the pore. The current is then found by the integration $I = \int F(J_{Cl} + J_K)dA$, where F is the Faraday constant, A is the cross-sectional area of the pore with or without DNA, J_{Cl} is chloride ion's flux, and

J_K is potassium ion's flux. Fully solving for current in this way considers the access resistance of the nanopore,[33,40] as well as the geometry of the tapered nanopore wall shown in Figure 1c. The detailed calculation of current passing through a nanopore is explained in our earlier report.[33]

In this simulation, a double-stranded DNA molecule was assumed to be a 2.2 nm diameter rigid cylinder, and the thickness profile data in Figure 1c for the geometries of a nanopore and free-standing membrane were used. To match the experimentally measured open pore current, a 26 nm diameter pore was used in this simulation. Figure 4b shows the amount of DNA-induced current drop as the DNA–nanopore distance changed. The insets in Figure 4 show two of the DNA–nanopore configurations for the simulation. The DNA–nanopore distance in Figure 4b is defined from membrane's top surface to the DNA cylinder's front end. The current blockage started when the front end of the DNA was about 50 nm above the nanopore (top left, Figure 4b), consistent with the concept of nanopore access resistance. The current blockage reached a maximum of 43 pA when the cylinder's bottom is 200 nm below the nanopore entrance, the very end of the FIB hole region. This value matches to the right peak in Figure 4a of the experimental data. When the DNA cylinder's front end is right above the nanopore, the current blockage is 25 pA. Based on these two current blockage numbers, a possible interpretation is that the left peak in Figure 4a is related to DNA's sticking to the nanopore's entrance without translocating. This is also consistent with many DNA sticking or collision events observed during solid-state nanopore experiments when tether-free DNA was used in our lab (data not shown) and reported by other groups.[41]

The above simulation is based on the idea that volume exclusion is the only mechanism for DNA-induced current blockades ΔI_b. Earlier reports have shown that other parameters also contribute to the magnitude of current blockades. Reiner *et al.*[42] proposed that the ionic current can be reduced not only by DNA volume exclusion but also by ion exclusion due to cation binding to DNA inside a pore. To further understand and more precisely calculate the interactions of a DNA molecule with a nanopore in our future experiments, Reiner's proposal may be necessary. Furthermore, we have also ignored how asymmetrical charge distribution influences ionic current through a nanopore as reported in a study of protein pores.[43] Based on our previous study, the surface charge's influence on the ionic current through a 25 nm diameter nanopore in 1 M KCl was negligible.[33] Therefore, we did not consider the nanopore's surface charge effects on current blockade caused by DNA translocation through a pore. In summary, the absolute DNA-blocked current could also be dependent on the pore geometry, ion binding to DNA, as well as surface charge on a nanopore. In this simulation, we consider only the volume exclusion to provide qualitative values of blocked current ΔI_b as a function of DNA–nanopore position (Figure 4b) to estimate the DNA–nanopore configuration.

To further verify that the current drop and recovery steps were produced by DNA molecules interacting with a nanopore, we have attached both ends of biotinylated λ DNA molecules to the probe tip. In addition to the current drop and recovery steps observed in Figure 4b, larger current drop and recovery steps were observed (see Figures SI_10 and 11). The current blockage histogram using the both ends biotinylated is shown in Figure 5. As we expected,

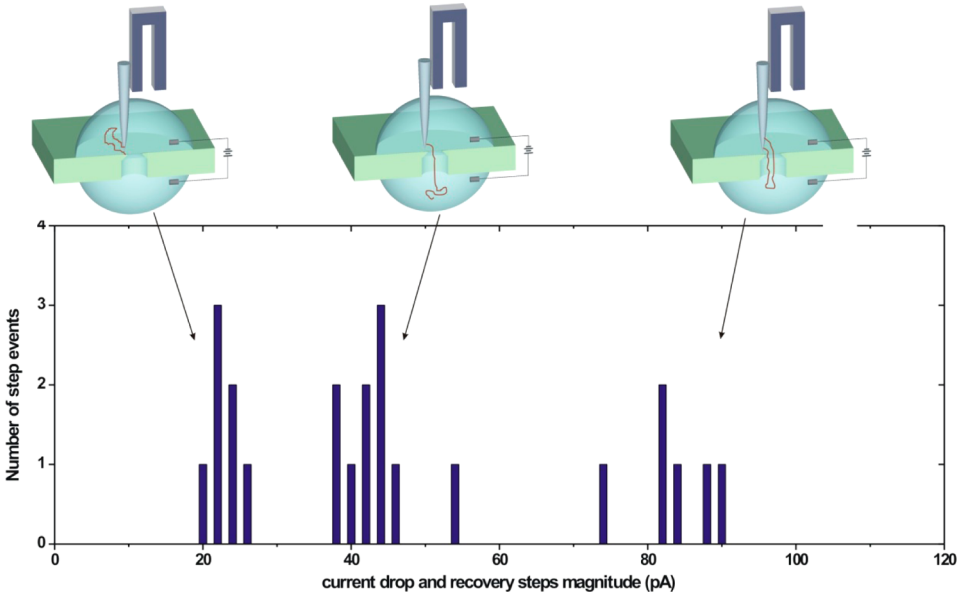

Figure 5. Current drop amplitudes when some of the λ DNA molecules are biotinylated at both ends. Two sets of data were recorded from two nanopores. One had an open pore current I_0 = 23.4 nA, and the other had I_0 = 13.0 nA.

the current blockage histogram shows three distinctive groups. The left group has $\Delta I_1 = 22.9 \pm 2.0$ pA, possibly corresponding to DNA's incomplete translocation as depicted on top left of Figure 5. The center group has $\Delta I_2 = 43.8 \pm 4.5$ pA, possibly related to one λ dsDNA translocation with only one end anchored to the tip. The right group has $\Delta I_3 = 83.3 \pm 5.6$ pA, which would match a double-anchored λ DNA as shown on the top right of Figure 5. This further demonstrates that the 43.8 pA current drop is most likely caused by a dsDNA translocation in the pore. Shorter release distances expected for a double-anchored λ DNA were not consistently observed. A possible explanation is that a U-shaped DNA molecule is difficult to pull out due to the pore−DNA interaction, thus often broke off from the tip and trapped in the pore as we observed (see Figures SI_10 and SI_11).

CONCLUSION

In this work, we report a novel method that is capable of controlling DNA translocation speed in a solid-state nanopore to the order of ~100 μs/base by tethering λ DNA molecules to a probe tip. The tip's position is sensed and controlled by a tuning fork based force sensor and by a nanopositioning system. This SSN-TFFSP system can bring a DNA-tethered TFFSP tip close to a nanopore, monitor the capture process of a DNA molecule by a voltage-biased nanopore, and most importantly, pull a captured and trapped DNA out of the nanopore with controlled speed and subnanometer accuracy. The measured DNA's capture and release distances are comparable to the gyration diameter and the contour length of the 48.5 kb λ DNA respectively. The recorded current signals show the expected current drop and recovery steps for one end and for both ends biotinylated λ DNA molecules. In addition, current traces also revealed that some DNA molecules did not translocate completely through a nanopore, but they stayed near the nanopore's entrance. This was also supported by finite element analysis computer simulation. This SSN-TFFSP system has demonstrated the capability of slowing down DNA moving speed in a pore more than 1000 times compared to tether-free DNA translocation through solid-state nanopores, which allows studying DNA−nanopore interaction in great detail and provides enough temporal resolution to read each base on a tethered DNA molecule in the future.

Furthermore, this system potentially can have many other applications in the field of manipulation and detection of single DNA and protein molecules. The SSN-TFFSP system has the following advantages: controlling the motion of biomolecules at angstrom precision with user-defined moving speed, characterizing single DNA and protein molecules with solid-state nanopores and possibly protein pores, and using very small number of biomolecules. A few such examples of its applications include measuring DNA hybridization, RNA−protein and DNA−protein interactions, and single-protein molecules in nanopores.

METHODS

The quartz tuning fork (Fox Electronics, NC38LF-327) shown in Figure 1a is used as a force feedback sensor as demonstrated by other reports.[44,45] By attaching a tip to one prong of a tuning fork, this device can be used as a force feedback sensor.[46,47] The detailed tuning fork setup is reported in our other work.[48] Briefly, at the resonance frequency, the vibration of the quartz tuning fork generates a small voltage, a few millivolts. This vibration amplitude is sensitive to the viscous drag in solution and the shear force when the tip is close to a surface. This voltage signal is 1000 times preamplified, and its amplitude is measured by a lock-in amplifier (Stanford Research Systems, SR850). The same lock-in amplifier is also used to generate the driving voltage for the piezo actuator. The oscillation amplitude of the tuning fork estimates that the output voltage/displacement is 0.18 mV/nm by considering quartz's properties and the tuning fork's geometry.[48,49]

The probe tip is made from a single-mode optical fiber (Corning Optical fiber, SMF-28(TM)) using a micropipet puller (Sutter Instrument, P-2000). The pulled fiber tip is cleaned by Piranha solution (sulfuric acid/hydrogen peroxide = 3:1) for 10 min and then washed with DI water. The tip is coated with 250 nm thick chromium and gold using a sputter coater (Cressington, 108 auto). A typical Cr/Au-coated tip used in this report is shown in Figure 1d.

The nanopores used in this study are fabricated in a free-standing low-stress silicon nitride membrane supported by a silicon substrate as described previously.[2] The silicon-rich, low-stress silicon nitride membrane (~275 nm in thickness) was deposited by low-pressure chemical vapor deposition (LPCVD) on both sides of the silicon substrate. One side of the silicon nitride membrane window is opened by procedures including photolithography, reactive ion etching, and anisotropic wet KOH etching to produce a free-standing silicon nitride membrane. A cavity of about 100 nm size is milled on the free-standing membrane window with a focused ion beam (FIB, Micrion 9500) machine, leaving a tapered membrane with a thickness of 20−30 nm. Then a nanopore is drilled in the cavity using a high-energy electron beam in a TEM (300 keV FEI Titan). The thickness profile across the nanopore in Figure 1c was measured by taking the log-ratio of an energy-filtered zero-loss TEM image and unfiltered TEM image of the nanopore with $T = \lambda \ln(I_1/I_0)$,[50] where λ, I_1, and I_0 are inelastic mean free path, unfiltered image intensity, and zero-loss intensity, respectively. The mean free path λ is calculated empirically by measuring the thickness of the membrane using a standard optical reflectometer. We found λ at 300 keV to be 180 nm with errors of approximately 10%. According to the thickness measurement, the silicon nitride membrane window is typically 210 nm thick and the cavity region is tapered to the nanopore by approximately 45°.

The λ DNA (NEB, N3011S) are biotinylated following the procedures described by Keyser *et al.*[18] The one end biotinylated oligonucleotides (Integrated DNA Technologies) matching the known "overhang" sequence of λ DNA were purchased. The λ DNA and the biotinylated oligonucleotides were ligated with T4 ligase enzyme (NEB). A DNA extraction kit (QIAGEN, QIAEX II gel extraction kit) was used to purify the biotinylated λ DNA after the ligation.

Attaching Biotinylated λ DNA to the Tip. The Cr/Au-coated optical fiber tip was immersed in a 10 mg/mL streptavidin (Invitrogen, 434301) solution for 10 min. The depth of the tip in the solution was about 10−20 μm. Streptavidin protein molecules were

adsorbed to the Au-coated tip during this process. The tip was then washed by DI water a few times to remove weakly adsorbed streptavidin. Fluorescently labeled streptavidin was used to verify the adsorption. The streptavidin-adsorbed tip was then soaked in the biotin-labeled λ DNA (~2 nM) for 10 min. After soaking the tip in the λ DNA solution, the tip's end was kept in 1 M KCl solution during the experiment to avoid the detachment of DNA from the tip. To verify that the λ DNA molecules were attached to the tip by this method, we further performed experiments to stretch the tethered DNA molecules by an AC electric field in salt solution under a fluorescent microscope.[48] The fluorescent images had shown that many copies of λ DNA molecules are attached to the end of a tip by this procedure.

Conflict of Interest: The authors declare no competing financial interest.

Acknowledgment. The authors thank Professor J. Golovchenko's nanopore group for FIB pore preparation, D. Tita, S. Nandivada, and N. Walsh for nanopore fabrication, R.W. Penhallegon for electronics support, Dr. M. Benamara for TEM imaging, Dr. Tao Huang for helping setting up the instrument, and Prof. D. McNabb for helping DNA preparation. TEM-related work was performed at the Arkansas Nano-Bio Materials Characterization Facility. Support of this research has been provided by NHGRI/NIH R21HG004776 and partially supported by ABI1116.

Supporting Information Available: Additional data sets and figures are included in the Supporting Information. This material is available free of charge *via* the Internet at http://pubs.acs.org.

REFERENCES AND NOTES

1. Kasianowicz, J. J.; Brandin, E.; Branton, D.; Deamer, D. W. Characterization of Individual Polynucleotide Molecules Using a Membrane Channel. *Proc. Natl. Acad. Sci. U.S.A.* **1996**, *93*, 13770–13773.
2. Li, J.; Stein, D.; McMullan, C.; Branton, D.; Aziz, M. J.; Golovchenko, J. A. Ion-Beam Sculpting at Nanometre Length Scales. *Nature* **2001**, *412*, 166–169.
3. Storm, A. J.; Chen, J. H.; Ling, X. S.; Zandbergen, H. W.; Dekker, C. Fabrication of Solid-State Nanopores with Single-Nanometre Precision. *Nat. Mater.* **2003**, *2*, 537–540.
4. Li, J.; Gershow, M.; Stein, D.; Brandin, E.; Golovchenko, J. A. DNA Molecules and Configurations in a Solid-State Nanopore Microscope. *Nat. Mater.* **2003**, *2*, 611–615.
5. Branton, D.; Deamer, D. W.; Marziali, A.; Bayley, H.; Benner, S. A.; Butler, T.; Ventra, M. D.; Garaj, S.; Hibbs, A.; Huang, X.; *et al.* The Potential and Challenges of Nanopore Sequencing. *Nat. Biotechnol.* **2008**, *26*, 1146–1153.
6. Dekker, C. Solid-State Nanopores. *Nat. Nanotechnol* **2007**, *2*, 209–215.
7. Venkatesan, B. M.; Bashir, R. Nanopore Sensors for Nucleic Acid Analysis. *Nat. Nanotechnol.* **2011**, *6*, 615–624.
8. Fologea, D.; Ledden, B.; McNabb, D. S.; Li, J. Electrical Characterization of Protein Molecules in a Solid-State Nanopore. *Appl. Phys. Lett.* **2007**, *91*, 053901.
9. Oukhaled, G.; Mathe, J.; Biance, A.-L.; Bacri, L.; Betton, J.-M.; Lairez, D.; Pelta, J.; Auvray, L. Unfolding of Proteins and Long Transient Conformations Detected by Single Nanopore Recording. *Phys. Rev. Lett.* **2007**, *98*, 158101.
10. Firnkes, M.; Pedone, D.; Knezevic, J.; Döblinger, M.; Rant, U. Electrically Facilitated Translocations of Proteins through Silicon Nitride Nanopores: Conjoint and Competitive Action of Diffusion, Electrophoresis, and Electroosmosis. *Nano Lett.* **2010**, *10*, 2162–2167.
11. Niedzwiecki, D. J.; Grazul, J.; Movileanu, L. Single-Molecule Observation of Protein Adsorption onto an Inorganic Surface. *J. Am. Chem. Soc.* **2010**, *132*, 10816–10822.
12. Oukhaled, A.; Cressiot, B.; Bacri, L.; Pastoriza-Gallego, M.; Betton, J.-M.; Bourhis, E.; Jede, R.; Gierak, J.; Auvray, L.; Pelta, J. Dynamics of Completely Unfolded and Native Proteins through Solid-State Nanopores as a Function of Electric Driving Force. *ACS Nano* **2011**, *5*, 3628–3638.
13. Yusko, E. C.; Johnson, J. M.; Majd, S.; Prangkio, P.; Rollings, R. C.; Li, J.; Yang, J.; Mayer, M. Controlling the Translocation of Proteins through Nanopores with Bioinspired Fluid Walls. *Nat. Nanotechnol.* **2011**, 253–260.
14. Merstorf, C.; Cressiot, B.; Pastoriza-Gallego, M.; Oukhaled, A.; Betton, J. M.; Auvray, L.; Pelta, J. Wild Type, Mutant Protein Unfolding and Phase Transition Detected by Single-Nanopore Recording. *ACS Chem. Biol.* **2012**, *7*, 652–658.
15. Wei, R.; Gatterdam, V.; Wieneke, R.; Tampé, R.; Rant, U. Stochastic Sensing of Proteins with Receptor-Modified Solid-State Nanopores. *Nat. Nanotechnol.* **2012**, *7*, 257–263.
16. Cressiot, B.; Oukhaled, A.; Patriarche, G.; Pastoriza-Gallego, M.; Betton, J.; Auvray, L.; Muthukumar, M.; Bacri, L.; Pelta, J. Protein Transport through a Narrow Solid-State Nanopore at High Voltage: Experiments and Theory. *ACS Nano* **2012**, *6*, 6236–6243.
17. Fologea, D.; Uplinger, J.; Thomas, B.; McNabb, D. S.; Li, J. Slowing DNA Translocation in a Solid State Nanopore. *Nano Lett.* **2005**, *5*, 1734–1737.
18. Keyser, U. F.; van der Does, J.; Dekker, C.; Dekker, N. H. Inserting and Manipulating DNA in a Nanopore. In *Micro and Nano Technologies in Bioanalysis: Methods and Protocols*; Lee, J. W., Foote, R. S., Eds.; Humana Press: New York, 2009; pp 95–112.
19. Garaj, S.; Hubbard, W.; Reina, A.; Kong, J.; Branton, D.; Golovchenko, J. A. Graphene as a Sub-nanometer Trans-electrode Membrane. *Nature* **2010**, *467*, 190–193.
20. Merchant, C. A.; Healy, K.; Wanunu, M.; Ray, V.; Peterman, N.; Bartel, J.; Fischbein, M. D.; Venta, K.; Luo, Z.; Johnson, A. T. C.; *et al.* DNA Translocation through Graphene Nanopores. *Nano Lett.* **2010**, *10*, 2915–2921.
21. Schneider, G. F.; Kowalczyk, S. W.; Calado, V. E.; Pandraud, G.; Zandbergen, H. W.; Vandersypen, L. M. K.; Dekker, C. DNA Translocation through Graphene Nanopores. *Nano Lett.* **2010**, *10*, 3163–3167.
22. Keyser, U. F. Controlling Molecular Transport through Nanopores. *J. R. Soc. Interface* **2011**, *8*, 1369–1378.
23. Wanunu, M.; Bhattacharya, S.; Xie, Y.; Tor, Y.; Aksimentiev, A.; Drndic, M. Nanopore Analysis of Individual RNA/Antibiotic Complexes. *ACS Nano* **2011**, *5*, 9345–9353.
24. Rosenstein, A. K.; Wanunu, M.; Merchant, C. A.; Drndic, M.; Shepard, K. L. Integrated Nanopore Sensing Platform with Sub-microsecond Temporal Resolution. *Nat. Methods* **2012**, *9*, 487–492.
25. Kowalczyk, S. W.; Wells, D. B.; Aksimentiev, A.; Dekker, C. Slowing down DNA Translocation through a Nanopore in Lithium Chloride. *Nano Lett.* **2012**, *12*, 1038–1044.
26. Manrao, E. A.; Derrington, I. M.; Laszlo, A. H.; Langford, K. W.; Hopper, M. K.; Gillgren, N.; Pavlenok, M.; Niederweis, M.; Gundlach, J. H. Reading DNA at Single-Nucleotide Resolution with a Mutant MspA Nanopore and Phi29 DNA Polymerase. *Nat. Biotechnol.* **2012**, *30*, 349–353.
27. Iqbal, S. M.; Akin, D.; Bashir, R. Solid-State Nanopore Channels with DNA Selectivity. *Nat. Nanotechnol.* **2007**, *2*, 243–248.
28. Keyser, U. F.; Koeleman, B. N.; van Dorp, S.; Krapf, D.; Smeets, R. M.; Lemay, S. G.; Dekker, N. H.; Dekker, C. Direct Force Measurements on DNA in a Solid-State Nanopore. *Nat. Phys.* **2006**, *2*, 473–477.
29. Peng, H.; Ling, X. S. Reverse DNA Translocation through a Solid-State Nanopore by Magnetic Tweezers. *Nanotechnology* **2009**, *20*, 185101.
30. Keyser, U. F.; Krapf, D.; Koeleman, B. N.; Smeets, R. M.; Dekker, N. H.; Dekker, C. Nanopore Tomography of a Laser Focus. *Nano Lett.* **2005**, *5*, 2253–2256.
31. Smeets, R. M. M.; Keyser, U. F.; Wu, M. Y.; Dekker, N. H.; Dekker, C. Nanobubbles in Solid-State Nanopores. *Phys. Rev. Lett.* **2006**, *97*, 088101.
32. King, G. M.; Golovchenko, J. A. Probing Nanotube–Nanopore Interactions. *Phys. Rev. Lett.* **2005**, *95*, 216103.
33. Hyun, C.; Rollings, R.; Li, J. Probing Access Resistance of Solid-State Nanopores with a Scanning-Probe Microscope Tip. *Small* **2012**, *8*, 385–392.
34. Trepagnier, E. H.; Radenovic, A.; Sivak, D.; Geissler, P.; Liphardt, J. Controlling DNA Capture and Propagation

through Artificial Nanopores. *Nano Lett.* **2007**, *7*, 2824–2830.
35. Fologea, D.; Gershow, M.; Ledden, B.; McNabb, D. S.; Golovchenko, J. A.; Li, J. Detecting Single Stranded DNA with a Solid State Nanopore. *Nano Lett.* **2005**, *5*, 1905–1909.
36. Wanuu, M.; Morrison, W.; Rabin, Y.; Grosberg, A. Y.; Meller, A. Electrostatic Focusing of Unlabelled DNA into Nanoscale Pores Using Salt Gradient. *Nat. Nanotechnol.* **2009**, *5*, 160–165.
37. Ando, G.; Hyun, C.; Li, J.; Mitsui, T. Directly Observing the Motion of DNA Molecules near Solid-State Nanopores. *ACS Nano* **2012**, *6*, 10090–10097.
38. Tabard-Cossa, V.; Wiggin, M.; Trivedi, D.; Dwyer, N. N. J. J. R.; Marziali, A. Single-Molecule Bonds Characterized by Solid-State Nanopore Force Spectroscopy. *ACS Nano* **2009**, *3*, 3009–3014.
39. Keyser, U. F.; van der Does, J.; Dekker, C.; Dekker, N. H. Optical Tweezers for Force Measurements on DNA in Nanopores. *Rev. Sci. Instrum.* **2006**, *77*, 105105.
40. Hall, J. E. Access Resistance of a Small Circular Pore. *J. Gen. Physiol.* **1975**, *66*, 531–532.
41. van den Hout, M.; Krude, V.; Janssen, X. J. A.; Dekker, N. H. Distinguishable Populations Report on the Interactions of Single DNA Molecules with Solid-State Nanopores. *Biophys. J.* **2010**, *99*, 3840–3848.
42. Reiner, J. E.; Kasianowicz, J. J.; Nablo, B. J.; Robertson, J. W. F. Theory for Polymer Analysis Using Nanopore-Based Single-Molecule Mass Spectrometry. *Proc. Natl. Acad. Sci. U.S.A.* **2010**, *107*, 12080–12085.
43. Noskov, S. Y.; Im, W.; Roux, B. Ion Permeation through the α-Hemolysin Channel: Theoretical Studies Based on Brownian Dynamics and Poisson−Nernst−Plank Electrodiffusion Theory. *Biophys. J.* **2004**, *87*, 2299–2309.
44. Grober, R. D.; Acimovic, J.; Schuck, J.; Hessman, D.; Kindlemann, P. J.; Karrai, K.; Tiemann, I.; Manus, S. Fundamental Limits to Force Detection Using Quartz Tuning Forks. *Rev. Sci. Instrum.* **2000**, *71*, 2776–2780.
45. Friedt, J. M.; Barry, E. Introduction to the Quartz Tuning Fork. *Am. J. Phys.* **2007**, *75*, 415–422.
46. Edwards, H.; Taylor, L.; Duncan, W.; Melmed, A. J. Fast Low-Cost Phase Detection Setup for Tapping-Mode Atomic Force Microscopy. *Rev. Sci. Instrum.* **1997**, *70*, 3614–3619.
47. King, G. M.; Lamb, J. S.; Nunes, G. Quartz Tuning Forks as Sensors for Attractive-Mode Force Microscopy under Ambient Conditions. *Appl. Phys. Lett.* **2001**, *79*, 1712–1714.
48. Hyun, C.; Kaur, H.; McNabb, D. S.; Li, J. Stretching Tethered DNA on a SPM Tip by Dielectrophoresis. In preparation.
49. Kim, K.; Seo, Y.; Jang, H.; Chang, S.; Hong, M.-H.; Jhe, W. Shear-Mode Magnetic Force Microscopy with a Quartz Tunning Fork in Ambient Conditons. *Nanotechnology* **2006**, *17*, S201–S204.
50. Egerton, R. F. *Electron Energy-Loss Spectroscopy in the Electron Microscope*; Plenum Press: New York, 1996.